Articles

Anthanthrene Derivatives as Blue Emitting Materials for Organic Light-Emitting Diode Applications

Bipin K. Shah* and Douglas C. Neckers*

Center for Photochemical Sciences, Bowling Green State University, Bowling Green, Ohio 43403

Jianmin Shi,* Eric W. Forsythe, and David Morton

U.S. Army Research Laboratory, AMSRD-SE-EO, 2800 Power Mill Road, Adelphi, Maryland 20783

Received September 30, 2005. Revised Manuscript Received November 30, 2005

Photophysical properties of anthanthrene (**1**) and its derivatives (**2**−**11**) substituted at the 4,10 and/or 6,12 positions ($\phi_F = 0.25-0.56$, $\tau_F = 2.93-4.21$ ns in CH_2Cl_2) are compared. Solution emission behavior ($\lambda_{max} = 438-482$ nm) is similar to that observed in the solid state ($\lambda_{max} = 437-465$ nm). The compounds are shown to be efficient and very stable blue emitters, especially in the solid state ($\phi_F = 0.39-0.86$). An electroluminescent (EL) device containing **5** as a dopant produced an EL efficiency of 3.0 cd/A with CIE coordinates of 0.13 and 0.25. The luminescence half-life of the device was more than 3500 h with an initial luminescence ∼ 600 cd/m^2.

Introduction

Design and synthesis of blue emitting materials suitable for the fabrication of stable organic light-emitting diodes (OLEDs) is an active area of research.[1] Enormous effort has focused on the achievement of higher efficiency and longer operational stability in blue electroluminescent (EL) devices. Anthracene, one of the earliest reported luminescent materials, emits violet in the solid state and in solution. Derivatives such as 9,10-di-2-naphthylanthracene and 2-*tert*-butyl-9,10-di-2-naphthylanthracene (TBADN) doped with aggregation-resistant 2,5,8,11-tetra-*tert*-butylperylene (TBP) have been successfully used as blue emitters in commercial OLED products.[2]

On the basis of the efficiency reported and stability of anthracene derivatives, we have designed and synthesized a new class of blue emitters based on anthanthrene.[3] The emission characteristics of the anthanthrene derivatives that were substituted at 4,6,10,12 positions by the phenyl and *p*-*tert*-butylphenyl groups were recently reported.[4] These compounds showed blue fluorescence in solution ($\lambda_{max} = 437-467$ nm) with fluorescence quantum yields ($\phi_F = 0.24-0.33$ in CH_2Cl_2) ranging between those of anthracene (0.10 in CH_2Cl_2) and perylene (0.93 in CH_2Cl_2). Their radiative ($k_R \sim 8 \times 10^7$ s^{-1}) and nonradiative ($k_{NR} \sim 2.5 \times 10^8$ s^{-1}) rate constants of deactivation from the singlet surface were found to be similar to those reported for anthracene ($k_R \sim 6 \times 10^7$ s^{-1} and $k_{NR} \sim 2 \times 10^8$ s^{-1}).

To see the effect of various substituents on the properties of this class of compounds, new anthanthrene derivatives that have phenyl, *o*-tolyl, *p*-biphenyl, *p*-trifluoromethylphenyl, and 1-naphthyl substituents at the 4,10 and/or 6,12 positions of anthanthrene were synthesized and studied (Chart 1). Compounds **2**−**5** are 4,10 and 6,12-diphenyl substituted

Chart 1. Chemical Structures of Anthanthrene (1) and Substituted Anthanthrenes (2−11)

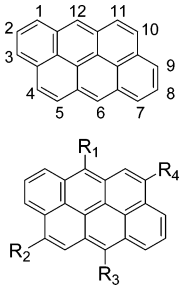

1. R_1, R_2, R_3, R_4 = H
2. R_1, R_3 = H; R_2, R_4 = phenyl
3. R_1, R_3 = phenyl; R_2, R_4 = H
4. R_1, R_2, R_3, R_4 = phenyl
5. R_1, R_2, R_3, R_4 = *p*-*tert*-butylphenyl
6. R_1, R_2, R_3 = H; R_4 = *o*-tolyl
7. R_1, R_3 = H; R_2, R_4 = *o*-tolyl
8. R_1, R_2, R_3, R_4 = *o*-tolyl
9. R_1, R_3 = 1-naphthyl; R_2, R_4 = *o*-tolyl
10. R_1, R_3 = *p*-trifluoromethylphneyl; R_2, R_4 = *o*-tolyl
11. R_1, R_3 = *p*-biphenyl; R_2, R_4 = *o*-tolyl

* To whom correspondence should be addressed. E-mail: bipin@bgnet.bgsu.edu (B.K.S.); neckers@photo.bgsu.edu (D.C.N.); jshi@arl.army.mil (J.S.).

(1) (a) Zheng, S.; Shi, J.; Mateu, R. *Chem. Mater.* **2000**, *12*, 1814. (b) Lee, S. H.; Nakamura, T.; Tsutsui, T. *Org. Lett.* **2001**, *3*, 2005. (c) Zheng, S.; Shi, J. *Chem. Mater.* **2001**, *13*, 4405. (d) Holmes, R. J.; D'Andrade, B. W.; Forrest, S. R.; Ren, X.; Li, J.; Thompson, M. E. *Appl. Phys. Lett.* **2003**, *83*, 3818. (e) Li, J.; Djurovich, P. I.; Alleyne, B. D.; Tsyba, I.; Ho, N. N.; Bau, R.; Thompson, M. E. *Polyhedron* **2004**, *23*, 419. (f) Hosokawa, C.; Fukuoka, K.; Kawamura, H.; Sakai, T.; Kubota, M.; Funahashi, M.; Moriwaki, F.; Ikeda, H. *SID04 Digest*; Society for Information Display: San Jose, CA, 2004; Vol. XXXV, p 780. (g) Li, Z. H.; Wong, M. S.; Tao, Y.; Lu, J. *Chem.—Eur. J.* **2005**, *11*, 3285. (h) Kulkarni, A. P.; Gifford, A. P.; Tonzola, C. J.; Jenekhe, S. A. *Appl. Phys. Lett.* **2005**, *86*, 061106/1.

(2) (a) Shi, J.; Tang, C. W.; Chen, C. U.S. Patent 6,720, 090, 2004. (b) Shi, J.; Tang, C. W. *Appl. Phys. Lett.* **2002**, *80*, 3201.

(3) (a) Shi, J.; Forsythe, E. W.; Morton, D. C. U.S. Patent Appl. 10/807,-099, 2004. (b) Shi, J.; Forsythe, E. W.; Morton, D. C. U.S. Patent Appl. 10/807,103, 2004.

(4) Shah, B. K.; Neckers, D. C.; Shi, J.; Forsythe, E. W.; Morton, D. *J. Phys. Chem. A* **2005**, *109*, 7677.

10.1021/cm052188x CCC: $33.50
Published on Web 01/12/2006

Table 1. Absorption Maxima (A_{max}), Emission Maxima (λ_{max}), Quantum Yields of Fluorescence (ϕ_F), Fluorescence Lifetimes (τ_F), and HOMO−LUMO Energy Gaps (E_{H-L}) of 1−11

	solution[a]				solid state[b]			
compound	A_{max} (nm)	λ_{max} (nm)	ϕ_F	τ_F (ns)	$\lambda_{exc.}$ (nm)	λ_{max} (nm)	ϕ_F	E_{H-L}[c]
			Phenyl Series					
1	308, 433	437	0.24 ± 0.01	3.06	385	432	0.66	2.88
2	317, 439	442	0.33 ± 0.01	4.21	390	439	0.49	2.84
3	314, 448	457	0.56 ± 0.02	3.68	395	453	0.86	2.82
4	322, 454	462	0.26 ± 0.02	2.97	400	459	0.43	2.78
5	324, 456	467	0.27 ± 0.01	3.01	410	468	0.47	2.77
			o-Tolyl Series					
6	312, 435	438	0.25 ± 0.02	3.03	385	437	0.39	2.88
7	315, 437	440	0.32 ± 0.02	3.28	395	438	0.41	2.87
8	319, 451	456	0.35 ± 0.04	2.95	430	451	0.65	2.81
9	321, 454	466	0.36 ± 0.01	2.93	425	458	0.63	2.81
10	321, 453	469	0.33 ± 0.01	3.08	430	464	0.54	
11	323, 460	468	0.27 ± 0.03	2.93	430	465	0.47	2.80

[a] Solvent = CH_2Cl_2. Excitation wavelength ($\lambda_{exc.}$) = 330 nm for measuring ϕ_F and τ_F. The decay was monitored at the corresponding λ_{max} for τ_F. The ϕ_F values are relative to that of 9,10-diphenylanthracene (0.9 in cyclohexane). The solution data of **1**, **2**, **4** and **5** are taken from ref 4. [b] PMMA was used as the matrix. The ϕ_F values are within the 15% error range. [c] Calculated using the density functional theory method [B3LYP/6-31G(d)].

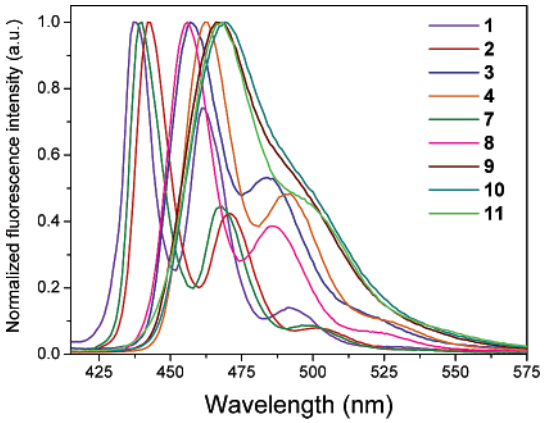

Figure 1. Normalized fluorescence spectra of **1**−**4** and **7**−**11** (~1×10^{-5} M) recorded in CH_2Cl_2.

and 4,6,10,12-tetraphenyl and *p*-*tert*-butylphenyl substituted anthanthrenes, while compounds **6**−**8** are *o*-tolyl derivatives and **9**−**11** are *o*-tolyl derivatives with different substituents at the 6,12 positions.

The detailed photophysical properties of **1**−**11** measured in solution (in CH_2Cl_2) are compared in this report. Their fluorescence efficiencies in the solid state [in poly(methyl methacrylate), PMMA, matrix] and the effects of aging and annealing on the solid-state emission behavior are evaluated. The performances of **2** and **5** in OLED devices are also discussed and are found to be as good as those of TBP.

Results and Discussion

Luminescene in Solution. The absorption spectra of **1**−**11** recorded in CH_2Cl_2 were almost similar in shape, showing a $\pi-\pi^*$ band at ~433−460 nm (see Supporting Information). The fluorescence spectra of **1**−**4** and **7**−**11** in CH_2Cl_2 (Figure 1) show the expected red shift in the emission of **2**−**11** compared to that of anthanthrene (**1**). This is attributed to an effective increase in the delocalization of π electrons in the molecules due to substitution.[4] The absorption maxima (A_{max}), emission maxima (λ_{max}), fluorescence quantum yields (ϕ_F), and lifetimes of fluorescence (τ_F) measured in CH_2Cl_2 are presented in Table 1.

It is noted that the red shift in λ_{max} from **1** to **2** (5 nm) or from **3** to **4** (5 nm) is smaller than that from **1** to **3** (20 nm), indicating a higher degree of delocalization of π electrons at the 6,12 positions than at the 4,10 positions. This may be associated with a higher degree of electron density at the 6,12 positions than at the 4,10 positions in anthanthrene. The higher reactivity at the 6,12 positions of anthanthrene seems analogous to the higher reactivity of the 9,10 positions of anthracene.

The ground-state structures of **4** and **8** optimized by the density functional theory method using B3LYP/6-31G* level of basis sets indicate that orthogonality between the anthanthrene core and the *o*-tolyl group is higher than that between the core and the phenyl groups. For example, the angle between the plane of the anthanthrene core and the plane of the *o*-tolyl group at either the 6 or the 12 position (89.9°) is higher than that between the plane of the core and the plane of the phenyl group at the 6 or 12 position (78.5°). This translates into a slight blue shift in the λ_{max} of *o*-tolyl susbstituted derivatives compared to that of the comparable phenyl derivatives; for example, the λ_{max} values of **7** (440 nm) and **8** (456 nm) are blue shifted compared to those of **2** (442 nm) and **4** (462 nm), respectively. 6,12-di-1-naphthyl (**9**), 6,12-di-*p*-trifluoromethylphenyl (**10**), and 6,12-di-*p*-biphenyl substituted (**11**) derivatives showed red shifted emission larger than that of other derivatives, although they have the *o*-tolyl group at the 4,10 positions. This may be the result of the presence of more conjugative groups at the 6,12 positions of these molecules.

The ϕ_F of **3** (0.56) measured in CH_2Cl_2 is higher among the phenyl series derivatives (**2**−**5**) and is much higher than that of **1** (0.24). Nevertheless, phenyl substitution at the 4,-10 or 4,6,10,12 positions results in the similar ϕ_F values of **2** and **4** (0.26 and 0.33, respectively) to that of **1**. The ϕ_F values of *o*-tolyl derivatives (**6**−**11**) were also found to be in the same range (0.25−0.36). Similar to the fluorescence decay of the phenyl derivatives,[4] the decay of fluorescence in the *o*-tolyl derivatives (**6**−**11**) could be satisfactorily fitted with monoexponential functions indicating emission from a single excited state (S_1 state) in each case. The τ_F values were found to be ~3−4 ns for each of the compounds. While the nonradiative rate constants of decay of the singlet states of **6**−**11** ($k_{NR} \sim 2 \times 10^8$ s^{-1}) were almost similar to those of **1** or anthracene ($k_{NR} \sim 2 \times 10^8$ s^{-1}), the radiative decay

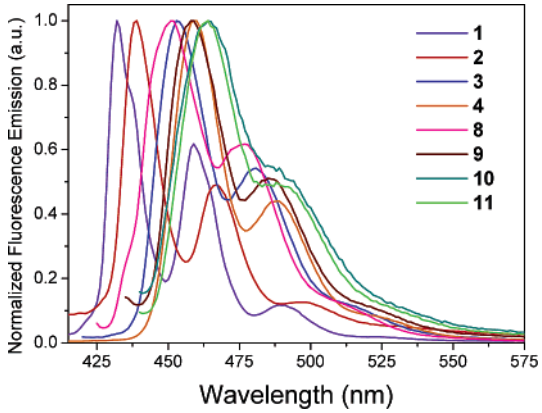

Figure 2. Normalized fluorescence spectra of **1**−**4** and **8**−**11** (~1×10^{-4} M) recorded in thin films of PMMA.

rate constants of the former ($k_R \sim 1 \times 10^8$ s^{-1}) were calculated to be slightly higher than those of **1** ($k_R \sim 8 \times 10^7$ s^{-1}) or anthracene ($k_R \sim 6 \times 10^7$ s^{-1}).[4,5]

Luminescene in the Solid State. The emission spectra of **1**−**4** and **8**−**11** recorded in thin films of PMMA are shown in Figure 2 (for clarity, the spectra of **5**−**7** are not shown). The solid-state emission spectra were similar to those recorded from the CH_2Cl_2 solution. Interestingly, the solid-state emission of each of the compounds was found to be slightly blue shifted (1−5 nm) from the corresponding solution emission. The trend toward a red shift in the solid-state emission among the phenyl and *o*-tolyl derivatives compared to that of **1** was similar to that observed in solution. The λ_{max} values of **2** and **3**, for example, are 7 and 21 nm more red shifted than that of **1**, respectively (Table 1). Similarly, the λ_{max} of **6** (437 nm) was the lowest and that of **11** (465 nm) was the highest among the *o*-tolyl derivatives.

The absolute solid state ϕ_F of **1**−**11** as measured using an integrating sphere are in the range of 0.39−0.86 (Table 1). The ϕ_F of **1** (0.66) obtained in a PMMA matrix was found to be similar to its absolute fluorescence quantum yield measured in benzene (0.62).[6] Under similar experimental conditions, the solid-state ϕ_F values of anthracene (0.23) and 9,10-diphenylanthracene (0.94) were also found to be similar to their reported absolute ϕ_F values in solution.[6] Although it is difficult to directly compare the absolute ϕ_F values of **1**−**11** measured in the solid state with their relative ϕ_F values measured in CH_2Cl_2 against 9,10-diphenylanthracene, it appears that the former is higher than the latter for each of the compounds. The electroluminescence (EL) efficiencies of **2** and **5** were also observed to be as high as that of TBP (vide infra). This may be explained on the basis of the similarities observed in the photophysical properties of anthracene and the anthanthrene derivatives.

There is relatively a large energy gap between the S_1 (3.1 eV) and T_1 (1.8 eV) states of anthracene.[7] It has been suggested that the presence of a T_2 state that is almost isoenergetic with the S_1 state provides a facile pathway for intersystem crossing in anthracene in solution, causing the molecule to lose the majority of its excited-state energy in

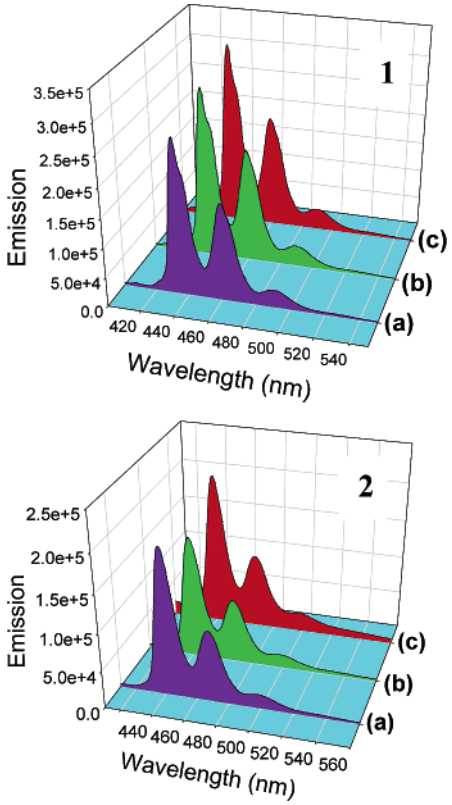

Figure 3. Fluorescence spectra recorded from thin films of PMMA containing **1** and **2**: (a) pristine, (b) after exposing the film for 7 days at ambient conditions, and (c) after heating the film at 150 °C for 24 h and cooling to room temperature.

dark processes via the T_2 and T_1 states.[8] A similar situation may pertain with the anthanthrene derivatives in solution. However, in the solid state the configuration of excited states of these molecules may be as such that the T_2 state is slightly higher in energy than the S_1 state, minimizing the S_1-T_2 intersystem crossing process. In such a case, energy transfer from the S_1 state to the T_1 state would not be an efficient process because of the reasonably high difference in the energy between the S_1 state and the T_1 state. This would cause an enhanced fluorescence in the solid state as observed experimentally.

Effect of Aging and Annealing on the Solid-State Emission. To evaluate the effect of aging and annealing on the solid-state emission behavior of the anthanthrene derivatives, emission spectra were recorded from the thin films of PMMA containing the sample which had been exposed to the ambient light at room temperature for 7 days and heated at 150 °C for 24 h. The emission spectra of **1**, **2**, and **5** remained the same after either treatment (shown for **1** and **2** in Figure 3), indicating that these compounds preserve their color purity under the conditions used for aging and annealing. This also demonstrates the stability of these compounds in the solid state.

EL and Device Performances. OLEDs were fabricated at 10^{-6} Torr in a deposition tool integrated with an inert atmosphere glovebox following a standard procedure. Indium tin oxide (ITO) was used as the anode, while 4,4′-bis[*N*-(1-

(5) Birks, J. B. *Photophysics of Aromatic Molecules*; Wiley−Interscience: New York, 1970; p 178.
(6) Dawson, W. R.; Windsor, M. W. *J. Phys. Chem.* **1968**, *72*, 3251.
(7) Schwob, H. P.; Williams, D. F. *J. Chem. Phys.* **1973**, *58*, 1542.
(8) Turro, N. J. *Modern Molecular Photochemistry*; University Science Books: Mill Valley, CA, 1991; p 187.

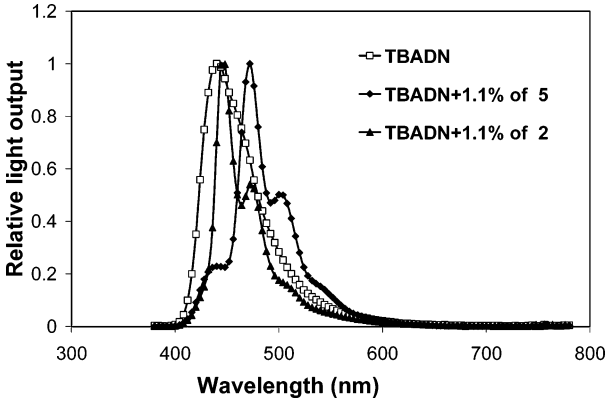

Figure 4. EL spectra of the TBADN EL devices undoped and doped with **2** and **5**.

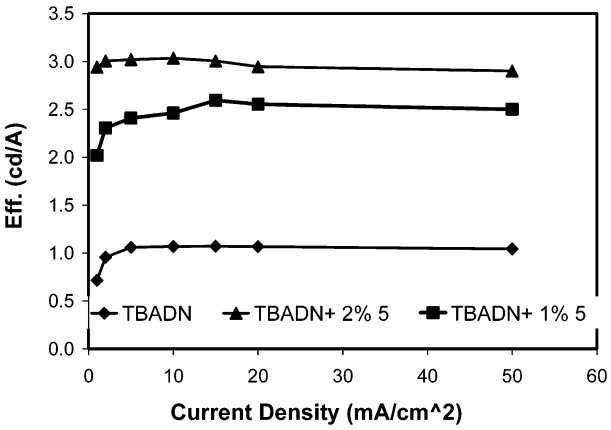

Figure 5. Dependence of the luminescence efficiency on the drive density for the TBADN EL devices undoped and doped with **5**.

naphthyl)-*N*-phenylamino]biphenyl (NPB) and tris(8-hydroxyquinolinato)aluminum (Alq) were used as the hole and electron transporting layers, respectively. The devices were fabricated with TBADN doped with **2** and **5** as the emissive layer. The former was used as the host material because of its known excited-state energy transfer property.[2] A device consisting of undoped TBADN as the emissive layer was studied for comparison. The OLED device structure and thicknesses of different layers were as follows: ITO/NPB ~500 Å/doped TBADN ~300 Å/Alq ~400 Å/MgAg ~2000 Å.

The EL emission spectrum of the undoped cell was broad, and centered at about 440 nm (Figure 4). The EL device doped with **5** showed an emission spectrum with narrow vibronic features that were characteristics of emission from **5**. Peak emission was centered at 472 nm, and the CIE coordinates were measured to be 0.13 and 0.25. The blue color was more saturated in the case of emission from the EL device doped with **2**. In this case, peak emission was centered at 446 nm, and the CIE coordinates were 0.15 and 0.14. The EL efficiencies of these anthanthrene derivative doped EL devices were satisfactorily high. For example, the EL efficiency of the device doped with 2% **5** (~3 cd/A) is similar to that observed for the TBP doped EL device (~3 cd/A).[2]

Figure 5 shows the dependence of the EL efficiency on the drive current density for the EL devices doped with **5**. The efficiency of the **5** doped EL devices was higher than that of the undoped device. When the concentration of **5** was increased from 1 to 2%, the EL efficiency slightly increased. However, an attempt to find out the optimal concentration for the highest EL efficiency was not made. It is noted that the efficiency of the 2% **5** doped EL device rose sharply at low current densities to a maximum of about 3.0 cd/A at about 5−20 mA/cm^2. There were no significant fall offs at higher current densities of either of the two **5** doped EL devices. The stability of these blue EL devices was tested under a direct current drive condition with the forward bias current maintained at 20 mA/cm^2. The luminance half-life was found to be more than 3500 h with an initial luminance around 600 cd/m^2.

Experimental Section

Solvents and reagents were used as received from commercial suppliers. $Pd(PPh_3)_4$ and **1** were purchased from Strem Chemicals and AccuStandard, respectively. Standard grade silica gel (60 Å, 32−63 μm) and silica gel plates (200 μm) were purchased from Sorbent Technologies. Reactions that required anhydrous conditions were carried out under argon in oven-dried glassware. Tetrahydrofuran (THF) and CH_2Cl_2 were distilled under argon from K−Na alloy and CaH_2, respectively.

Mass spectra were recorded on a Shimadzu GCMS-QP5050A instrument equipped with a direct probe (ionization 70 eV). Matrix assisted laser desorption ionization (MALDI) spectra were obtained using Bruker Daltonic Omniflex instrument (N_2 laser, 337 nm). A Bruker spectrometer (working frequency 300.0 MHz for ^{1}H) was used to record the NMR spectra. $CDCl_3$ was the solvent for NMR, and chemical shifts relative to tetramethylsilane at 0.00 ppm are reported in parts per million (ppm) on the δ scale. Absorption and fluorescence spectra were recorded on a Shimadzu UV-2401 spectrophotometer and a Fluorolog-3 spectrometer, respectively. All measurements were carried out at room temperature unless otherwise specified.

Synthesis. All anthanthrene derivatives (**2**−**11**, except **3**) were synthesized according to the general synthetic procedure described earlier,[4] using 4,9-dibromoanthanthrone and appropriate arylboronic acids. The characterization data of **2**, **4**, and **5** were also provided earlier.[4] Synthesis of **3** involved the cyclization of 1,1′-dinaphthyl-8,8′-dicarboxylic acid into anthanthrone, which was carried out following a literature procedure.[9] Anthanthrone was converted into **3** as follows: a fine suspension of anthanthrone (1 mmol, 0.3 g) in THF (~250 mL) was made by stirring the mixture overnight. The mixture was cooled to −78 °C, after which a solution of phenyllithium (1.9 M in cyclohexanes−ether, ~3 mmol) was added slowly not allowing the temperature to rise above −75 °C. After the addition was complete (~1 h), the resulting brown mixture was brought to room temperature and stirred for 3 h. The mixture was evaporated, and the resulting brown solid was subjected to the next step without further purification. Acetic acid (~10 mL) and hydriodic acid (55%, 1.5 mL) were added to the solid, and the mixture was refluxed for 2 h. The reaction mixture was cooled, water (~15 mL) was added, and then the mixture was extracted with CH_2Cl_2 (~50 mL × 4). The combined organic layers were evaporated to get crude **3**, which was further purified by repeated column chromatography using the solvent system used for other anthanthrene derivatives. **3** (0.14 g, yield ~ 30%) was recovered in the form of a white-yellow solid.

6,12-Diphenylanthanthrene (3). ^{1}H NMR (300 MHz, $CDCl_3$): δ 7.55−7.64 (m, 6H), 7.79 (d, 4H), 8.10 (t, 2H), 8.16 (s, 2H), 8.25

(9) Ansell, L. L.; Rangarajan, T.; Burgess, W. M.; Eisenbraun, E. J. *Org. Prep. Proced. Int.* **1976**, *8*, 133.

(d, 2H), 8.58 (d, 2H), 8.88 (s, 2H). MS (MALDI): calcd for $C_{34}H_{20}$, 428.2; found, 428.2 ($[M]^+$, 100%). MS (DIP) *m*/*z*: 428 (100) $[M]^+$, 350 (31), 212 (45), 175 (42).

4-*o*-Tolylanthanthrene (6). ^{1}H NMR (300 MHz, $CDCl_3$): δ 2.21 (s, 3H), 7.41−7.56 (m, 4H), 7.81 (d, 1H), 8.02−8.27 (m, 6H), 8.58 (d, 2H), 8.82 (d, 2H). MS (MALDI): calcd for $C_{29}H_{18}$, 366.1; found, 366.2 ($[M]^+$, 100%). MS (DIP) *m*/*z*: 366 (100) $[M]^+$, 350 (12), 175 (81).

4,10-Di-*o*-tolylanthanthrene (7). ^{1}H NMR (300 MHz, $CDCl_3$): δ 2.21 (s, 3H), 2.23 (s, 3H), 7.40−7.56 (m, 8H), 7.81 (d, 2H), 8.01−8.11 (m, 4H), 8.59 (d, 2H), 8.85 (s, 2H). MS (MALDI): calcd for $C_{36}H_{24}$, 456.2; found, 456.3 ($[M]^+$, 100%). MS (DIP) *m*/*z*: 456 (100) $[M]^+$, 363 (14), 212 (36).

4,6,10,12-Tetra-*o*-tolylanthanthrene (8). ^{1}H NMR (300 MHz, $CDCl_3$): δ 2.01−2.17 (m, 12H), 7.31−7.53 (m, 16H), 7.67 (s, 4H), 7.89 (d, 2H), 8.06 (d, 2H). MS (MALDI): calcd for $C_{50}H_{36}$, 636.3; found, 636.4 ($[M]^+$, 100%). MS (DIP) *m*/*z*: 636 (100) $[M]^+$, 546 (57), 256 (41), 219 (39).

4,10-Di-*o*-tolyl-6,12-di-1-naphthylanthanthrene (9). ^{1}H NMR (300 MHz, $CDCl_3$): δ 2.21 (d, 6H), 7.32−7.58 (m, 8H), 7.68−8.12 (m, 20H), 8.31 (s, 2H). MS (MALDI): calcd for $C_{56}H_{36}$, 708.3; found, 708.5 ($[M]^+$, 100%). MS (DIP) *m*/*z*: 709 (100) $[M]^+$, 616 (9), 354 (16).

4,10-Di-*o*-tolyl-6,12-di-*p*-trifluoromethylphenylanthanthrene (10). ^{1}H NMR (300 MHz, $CDCl_3$): δ 2.17 (d, 6H), 7.36−7.47 (m, 8H), 7.72−8.09 (m, 14H), 8.90 (s, 2H). MS (MALDI): calcd for $C_{50}H_{30}F_6$, 744.2; found, 744.5 ($[M]^+$, 100%). MS (DIP) *m*/*z*: 744 (100) $[M]^+$, 600 (83), 219 (56).

4,10-Di-*o*-tolyl-6,12-di-*p*-biphenylanthanthrene (11). ^{1}H NMR (300 MHz, $CDCl_3$): δ 2.18 (d, 6H), 7.37−7.57 (m, 14H), 7.68−7.99 (m, 18H), 8.26 (d, 2H). MS (MALDI): calcd for $C_{60}H_{40}$, 760.3; found, 760.5 ($[M]^+$, 100%). MS (DIP) *m*/*z*: 760 (100) $[M]^+$, 350 (33), 212 (46).

Fluorescence Quantum Yields (ϕ_F). Fluorescence quantum yields in solution were measured following a general method using 9,10-diphenylanthracene (ϕ_F = 0.9 in cyclohexane) as the standard.[10] Diluted solutions of **1**−**11** (10^{-5}−10^{-7} M) in appropriate solvents were used for recording the fluorescence spectra. Sample solutions were taken in quartz cuvettes and degassed for ∼15 min. The degassed solution had an absorbance of 0.04−0.06 at the excitation wavelength (330 nm). The fluorescence spectra of each of the sample solutions were recorded three times, and an average value of integrated areas of fluorescence was used for the calculation of ϕ_F. The refractive indices of solvents at the sodium D line were used.

ϕ_F values in the solid state were measured following a literature method.[11] A CH_2Cl_2 solution of sample was mixed with a concentrated solution of PMMA in acetonitrile in such a way that the overall concentration of the sample was $\sim 10^{-4}$ M. The resulting solution was cast into thin films on the quartz plates which were dried in oven at ∼100 °C for ∼1 h. The plate was inserted into an integrating sphere, and the required spectra were recorded.[11] The excitation wavelengths for **1**−**11** (Table 1) were selected on the basis of their absorption characteristics in the solid state. It is well know that, for molecules showing an overlap of absorption and emission spectra (a small Stokes shift), the use of an integrating sphere results in a substantial loss of emission due to reabsorption of the emitted light. To minimize the impact of this in the calculation of ϕ_F, the emission spectra of the PMMA films containing the sample were also recorded without using the integrating sphere. Comparing the solid-state emission spectra recorded with or without using the integrating sphere allowed the emission that was presumably lost as a result of the use of the integrating sphere to be recovered.

Fluorescence Lifetime (τ_F) Measurement. Solutions of **1**−**11** (10^{-4}−10^{-6} M in CH_2Cl_2) in quartz cuvettes showed absorbances of 0.07−0.1 at 330 nm. Fluorescence decay profiles of argon-degassed (∼15 min) solutions were recorded using a single photon counting spectrofluorimeter from Edinburgh Analytical Instruments (FL/FS 900). Decays were monitored at the emission maximum of the corresponding compounds. In-house-built software allowed the fitting of the decay spectra (χ^2 = 1.1−1.5) and yielded the fluorescence lifetimes.

Device Fabrication and EL Measurement. ITO was treated in an O_2 rf-plasma asher followed by CFx, which lowered the drive voltage by more than 2 V and made the current−voltage characteristics more consistent. Four substrates were loaded into a glovebox and transferred to the deposition chamber. The fabrication of the OLED device was carried out in a standard vacuum coater with a base pressure of about 10^{-6} Torr. The entire organic layer stack and the Mg:Ag cathode were deposited without a vacuum break to avoid exposure to the atmosphere. The deposition rate for organic layers was typically 4 Å/s, and for Mg:Ag it was 10 Å/s with a Mg-to-Ag ratio of 10:1.

The doped emissive layer was produced by co-depositing host TBADN and dopant simultaneously. The completed devices were transferred back to the glovebox and sealed with moisture absorbing material. The sealed devices were tested in air. The current−voltage characteristics were measured using a Keithley 2400 sourcemeter. The EL characteristics as a function of current density were measured with a PR650 spectrophotometer.

Geometry Optimization. The Gaussian 98 program package[12] was used for density functional theory calculations to optimize the geometries and calculate the highest occupied molecular orbital (HOMO) and lowest unoccupied molecular orbital (LUMO) energies.

Conclusions

Anthanthrene derivatives (**2**−**11**) substituted at the 4,10 and/or 6,12 positions by the phenyl, *o*-tolyl, *p*-*tert*-butylphenyl, 1-naphthyl, *p*-trifluoromethylphenyl, *p*-biphenyl groups were synthesized, and their photophysical properties (ϕ_F = 0.25−0.86, τ_F = 2.93−4.21 ns in CH_2Cl_2) were recorded. The degree of π electron delocalization was observed to be higher at the 6,12 positions than at the 4,10 positions. Their emission behaviors in CH_2Cl_2 (λ_{max} = 438−482 nm) and in the solid state (λ_{max} = 437−465 nm) were found to be similar. These compounds are good blue emitters in the solid state (absolute ϕ_F = 0.39−0.86 in the solid state). **1**, **2**, and

(10) Eaton, D. F. In *Handbook of Organic Photochemistry;* Scaiano, J. C., Ed.; CRC Press: Boca Raton, FL, 1989; Vol. I.

(11) (a) de Mello, J. C.; Wittmann, H. F.; Friend, R. H. *Adv. Mater.* **1997**, *9*, 230. (b) Pålsson, L. O.; Monkman, A. P. *Adv. Mater.* **2002**, *14*, 757.

(12) Frisch, M. J.; Trucks, G. W.; Schlegel, H. B.; Scuseria, G. E.; Robb, M. A.; Cheeseman, J. R.; Zakrzewski, V. G.; Montgomery, J. A., Jr.; Stratmann, R. E.; Burant, J. C.; Dapprich, S.; Millam, J. M.; Daniels, A. D.; Kudin, K. N.; Strain, M. C.; Farkas, O.; Tomasi, J.; Barone, V.; Cossi, M.; Cammi, R.; Mennucci, B.; Pomelli, C.; Adamo, C.; Clifford, S.; Ochterski, J.; Petersson, G. A.; Ayala, P. Y.; Cui, Q.; Morokuma, K.; Malick, D. K.; Rabuck, A. D.; Raghavachari, K.; Foresman, J. B.; Cioslowski, J.; Ortiz, J. V.; Stefanov, B. B.; Liu, G.; Liashenko, A.; Piskorz, P.; Komaromi, I.; Gomperts, R.; Martin, R. L.; Fox, D. J.; Keith, T.; Al-Laham, M. A.; Peng, C. Y.; Nanayakkara, A.; Gonzalez, C.; Challacombe, M.; Gill, P. M. W.; Johnson, B. G.; Chen, W.; Wong, M. W.; Andres, J. L.; Head-Gordon, M.; Replogle, E. S.; Pople, J. A. *Gaussian 98*, revision A.9; Gaussian, Inc.: Pittsburgh, PA, 1998.

5 retained the color integrity of their solid-state emission even when they were heated at 150 °C for 24 h or exposed to the ambient condition for 7 days. The EL device containing **2** as a dopant showed a saturated blue emission with CIE coordinates of 0.15 and 0.14. The EL efficiency of the device containing **5** as a dopant (3.0 cd/A) was similar to that shown by a TBP doped EL device (3.0 cd/A). The luminescence half-life of this device was more than 3500 h with an initial luminescence $\sim$ 600 cd/m^2.

Acknowledgment. We thank Dr. C. W. Tang for helpful discussions. We are pleased to acknowledge the support of the Army Research Laboratory (Contract No. DAAD19-03-2-0032).

Supporting Information Available: Absorption spectra of **3** and **6**−**11** recorded in CH_2Cl_2, some geometry optimized structures, and fluorescence decay profiles of **1**−**11** (PDF). This material is available free of charge via the Internet at http://pubs.acs.org.

CM052188X